

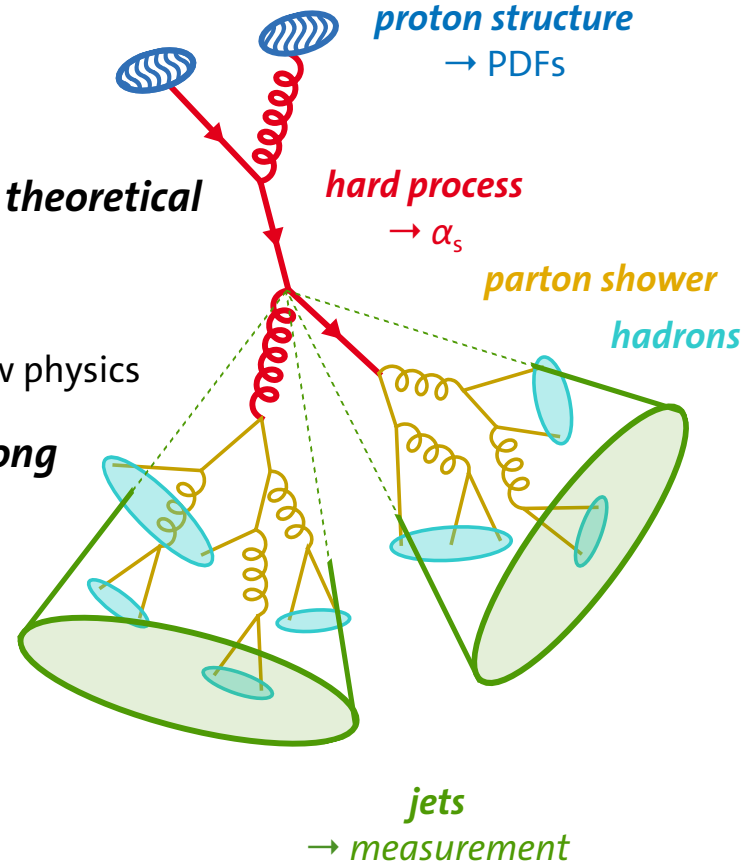
Jet measurements from CMS and ATLAS

New Trends in High-Energy and Low-x Physics | 2–5 September 2024 | Sfântu Gheorghe, Romania

Daniel Savoiu on behalf of the ATLAS and CMS collaborations

Why jets?

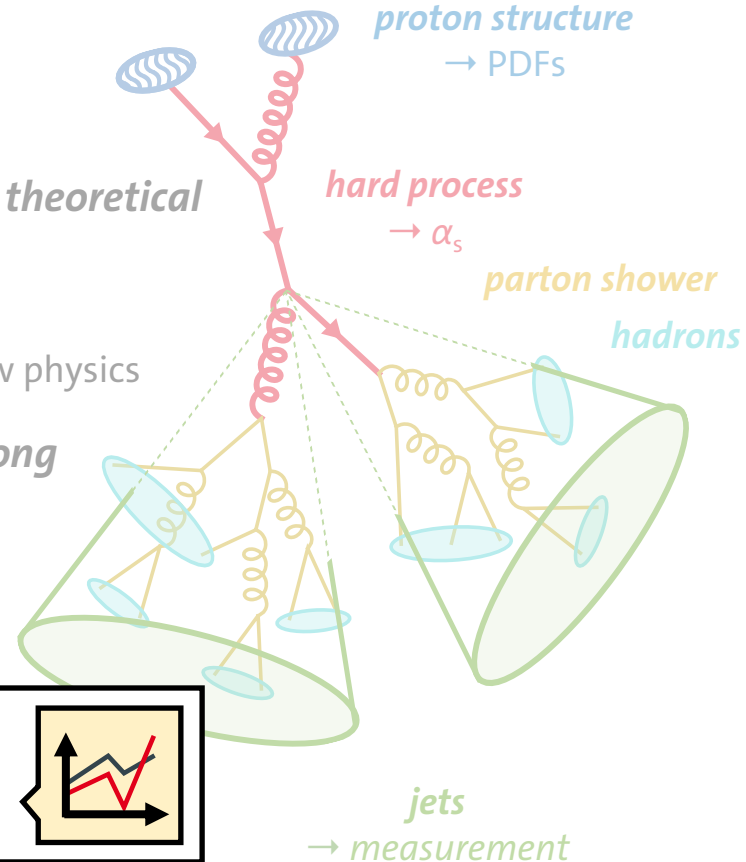
- jet production is dominant process at hadron colliders
- jet measurements provide essential input for improving **theoretical models** (perturbative QCD, parton showers, hadronization)
 - crucial for calculating any process at the LHC, precise modeling of background processes in searches for new physics
- esp. important for understanding **proton structure & strong interaction** (among theoretical components with largest uncertainties)
- rich measurement program at ATLAS & CMS + active theory community



Why jets?

- jet production is dominant process at hadron colliders
- jet measurements provide essential input for improving *theoretical models* (perturbative QCD, parton showers, hadronization)
 - crucial for calculating any process at the LHC, precise modeling of background processes in searches for new physics
- esp. important for understanding *proton structure & strong interaction* (among theoretical components with largest uncertainties)
- rich measurement program at ATLAS & CMS + active theory community

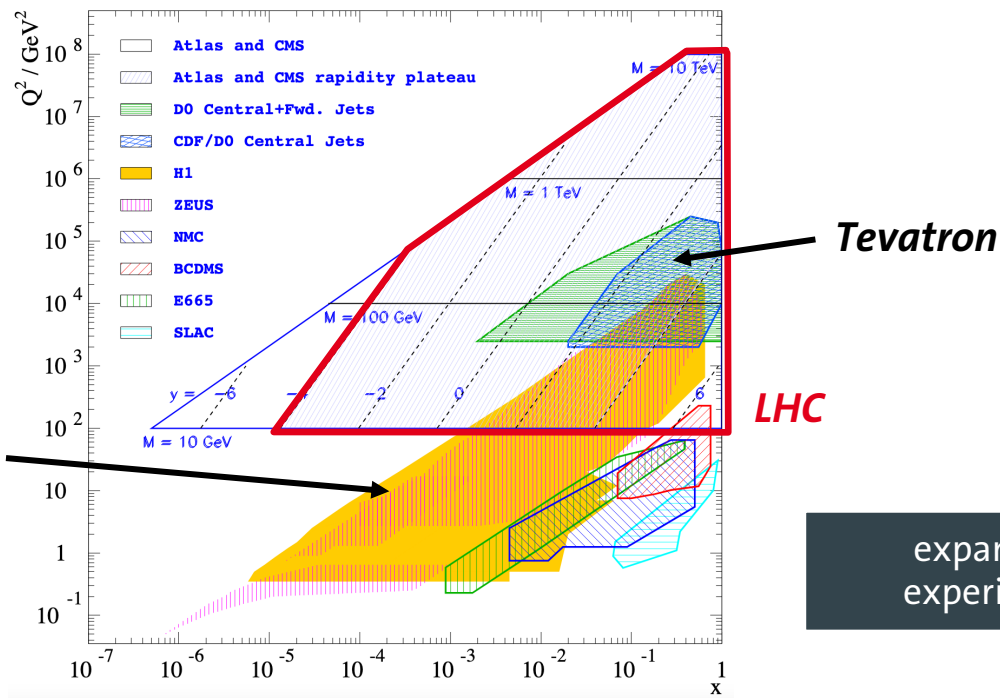
- *this talk*: personal highlights from recent results by both collaborations + attempt to identify *old & new trends*



Experimental reach in x and Q^2

phase spaces in parton momentum fraction x and energy scale Q^2 covered by experiments

HERA deep inelastic scattering (DIS) data

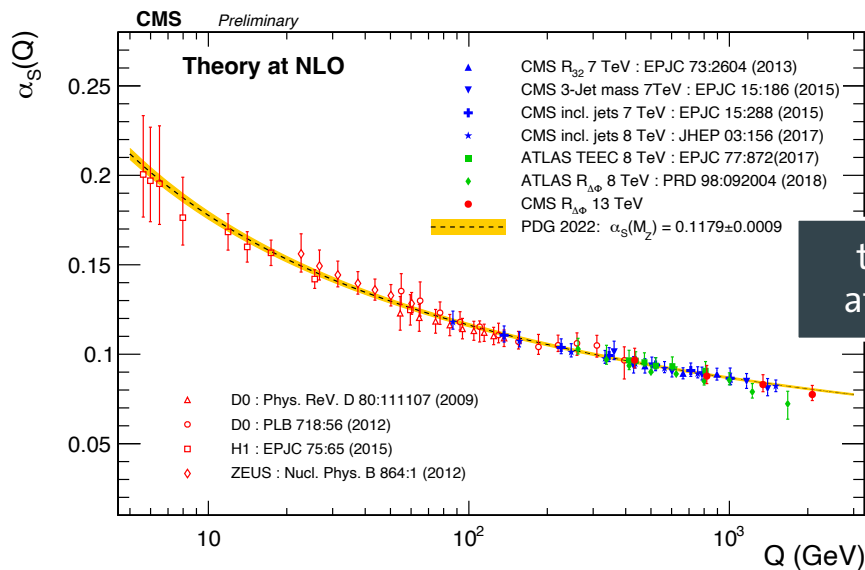


[D. South et al. "Review of Searches for Rare Processes and Physics Beyond the Standard Model at HERA", EPJ C 76 [doi:10.1140/epjc/s10052-016-4152-3](https://doi.org/10.1140/epjc/s10052-016-4152-3)]

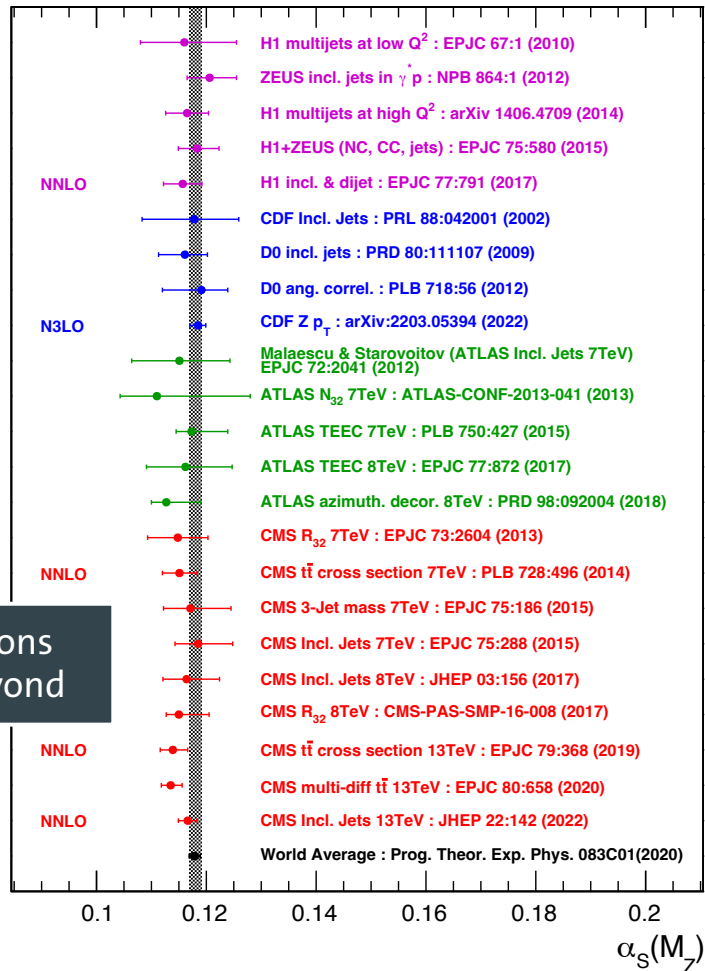
Sensitivity to the strong coupling

jet observables are naturally sensitive to *strong coupling* α_s

- precise determination of $\alpha_s(m_Z)$
- probe running of strong coupling at energies >1 TeV



theory calculations at NNLO and beyond



Selected results from ATLAS & CMS

Collab.	Title	Int. Lumi.	Energies (TeV)	Reference	arXiv
ATLAS	Measurement of inclusive jet and dijet production in pp collisions at $\sqrt{s} = 7$ TeV using the ATLAS detector	37 pb ⁻¹		7 PRD 86 (2012) 014022	1112.6297
CMS	Measurements of differential jet cross sections in proton-proton collisions at $\sqrt{s} = 7$ TeV with the CMS detector	5.0 fb ⁻¹		7 PRD 87 (2013) 112002	1212.6660
ATLAS	Measurement of the inclusive jet cross-section in proton-proton collisions at $\sqrt{s} = 7$ TeV using 4.5 fb ⁻¹ of data with the ATLAS detector	4.5 fb ⁻¹		7 JHEP 02 (2015) 153	1410.8857
CMS	Measurement and QCD analysis of double-differential inclusive jet cross-sections in pp collisions at $\sqrt{s} = 8$ TeV and ratios to 2.76 and 7 TeV	19.7 fb ⁻¹	2.76, 7, 8	JHEP 03 (2017) 156	1609.05331
CMS	Measurement of the triple-differential dijet cross section in proton-proton collisions at $\sqrt{s} = 8$ TeV and constraints on parton distribution functions	19.7 fb ⁻¹		8 EPJC 77 (2017) 11	1705.02628
ATLAS	Measurement of the inclusive jet cross-sections in proton-proton collisions at $\sqrt{s} = 8$ TeV with the ATLAS detector	20.2 fb ⁻¹		8 JHEP 09 (2017) 020	1706.03192
ATLAS	Measurement of inclusive jet and dijet cross-sections in proton-proton collisions at $\sqrt{s} = 13$ TeV with the ATLAS detector	3.2 fb ⁻¹		13 JHEP 05 (2018) 195	1711.02692
CMS	Measurement and QCD analysis of double-differential inclusive jet cross sections in proton-proton collisions at $\sqrt{s} = 13$ TeV	36.3 fb ⁻¹		13 JHEP 22 (2022) 142	2111.10431
CMS	Measurement of multidifferential cross sections for dijet production in proton-proton collisions at $\sqrt{s} = 13$ TeV	36.3 fb ⁻¹		13 Sub. EPJC	2312.16669
ATLAS	Measurements of jet cross-section ratios in 13 TeV proton-proton collisions with ATLAS	140 fb ⁻¹		13 Sub. PRD	2405.20206

Selected results from ATLAS & CMS

Collab.	Title	Int. Lumi.	Energies (TeV)	Reference	arXiv
ATLAS	Measurement of inclusive jet and dijet production in pp collisions at $\sqrt{s} = 7$ TeV using the ATLAS detector	37 pb ⁻¹		7 PRD 86 (2012) 014022	1112.6297
CMS	Measurements of differential jet cross sections in proton-proton collisions at $\sqrt{s} = 7$ TeV with the CMS detector	5.0 fb ⁻¹		7 PRD 87 (2012) 112002	1212.6660
ATLAS	Measurement of the inclusive jet cross-section in proton-proton collisions at $\sqrt{s} = 7$ TeV using 4.5 fb ⁻¹ of data with the ATLAS detector	4.5 fb ⁻¹		7 JHEP 02 (2015) 153	1410.8857
CMS	Measurement and QCD analysis of double-differential inclusive jet cross sections in pp collisions at $\sqrt{s} = 8$ TeV and ratios to 2.76 and 7 TeV	20.2 fb ⁻¹		7 JHEP 03 (2015) 037	1509.05531
CMS	Measurement of the triple-differential dijet cross section in proton-proton collisions at $\sqrt{s} = 8$ TeV and constraints on the distribution function	20.2 fb ⁻¹		8 EPJC 77 (2017) 11	1705.02628
ATLAS	Measurement of the inclusive jet cross-section in proton-proton collisions at $\sqrt{s} = 8$ TeV with the ATLAS detector	20.2 fb ⁻¹		8 JHEP 09 (2017) 020	1706.03192
ATLAS	Measurement of the inclusive jet cross-section in proton-proton collisions at $\sqrt{s} = 13$ TeV	3.2 fb ⁻¹		13 JHEP 05 (2018) 195	1711.02692
ATLAS	Measurement of the double-differential inclusive jet cross sections in proton-proton collisions at $\sqrt{s} = 13$ TeV	36.3 fb ⁻¹		13 JHEP 22 (2022) 142	2111.10431
CMS	Measurement of the multidifferential cross sections for dijet production in proton-proton collisions at $\sqrt{s} = 13$ TeV	36.3 fb ⁻¹		13 Sub. EPJC	2312.16669
ATLAS	Measurements of jet cross-section ratios in 13 TeV proton-proton collisions with ATLAS	140 fb ⁻¹		13 Sub. PRD	2405.20206

More results can be found on experiments' public information pages
<https://twiki.cern.ch/twiki/bin/view/AtlasPublic/StandardModelPublicResults>
<https://cms-results.web.cern.ch/cms-results/public-results/publications/SMP/index.html>

Observables

inclusive jet cross sections (“every jet counts”)

- direct probe of QCD at different scales and proton momentum fractions

dijet (+ trijet, ...) cross sections

- exploit jet topology for additional handle on PDFs over wide range in x

event shapes

- abstraction of topology beyond dijet allows constructing sensitive variables

jet substructure

- resolution of QCD processes inside jets

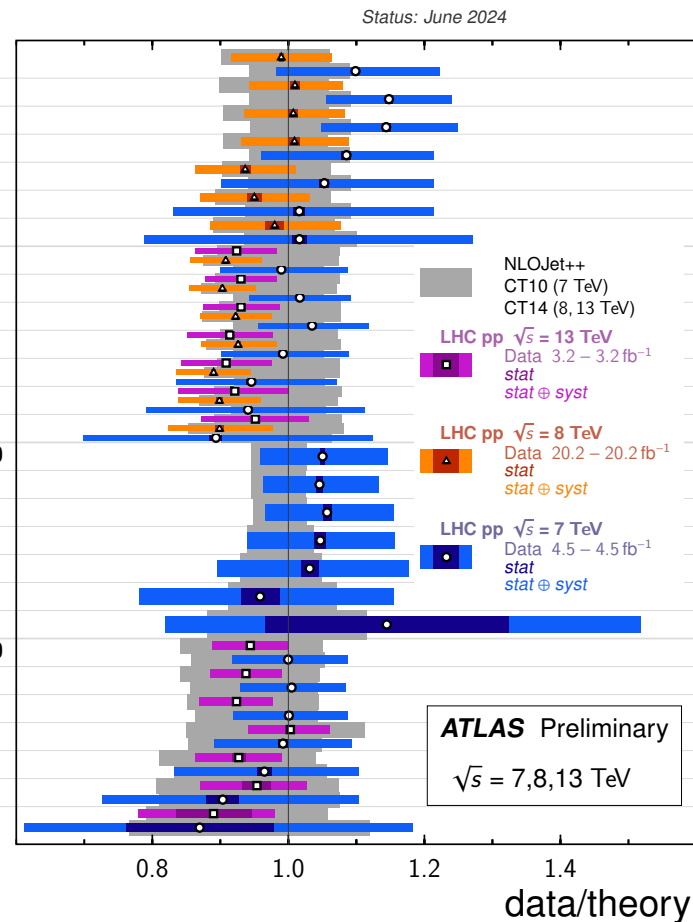


Incl. jet $R=0.6, |y| < 3.0$
 $-|y| < 0.5, p_T > 100 \text{ GeV}$
 $-0.5 < |y| < 1.0, p_T > 100 \text{ GeV}$
 $-1.0 < |y| < 1.5, p_T > 100 \text{ GeV}$
 $-1.5 < |y| < 2.0, p_T > 100 \text{ GeV}$
 $-2.0 < |y| < 2.5, p_T > 100 \text{ GeV}$
 $-2.5 < |y| < 3.0, p_T > 100 \text{ GeV}$

Incl. jet $R=0.4, |y| < 3.0$
 $-|y| < 0.5, p_T > 100 \text{ GeV}$
 $-0.5 < |y| < 1.0, p_T > 100 \text{ GeV}$
 $-1.0 < |y| < 1.5, p_T > 100 \text{ GeV}$
 $-1.5 < |y| < 2.0, p_T > 100 \text{ GeV}$
 $-2.0 < |y| < 2.5, p_T > 100 \text{ GeV}$
 $-2.5 < |y| < 3.0, p_T > 100 \text{ GeV}$

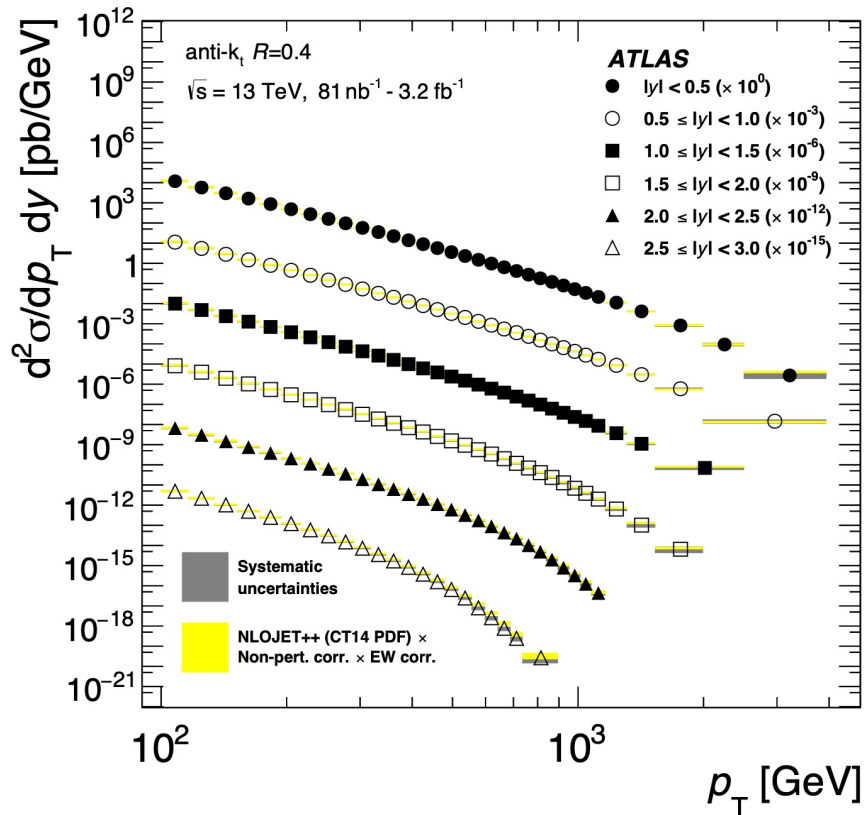
Dijet $R=0.6, |y| < 3.0, y^* < 3.0$
 $-y^* < 0.5, 0.3 < m_{jj} < 4.3 \text{ TeV}$
 $-0.5 < y^* < 1.0, 0.3 < m_{jj} < 4.3 \text{ TeV}$
 $-1.0 < y^* < 1.5, 0.5 < m_{jj} < 4.6 \text{ TeV}$
 $-1.5 < y^* < 2.0, 0.8 < m_{jj} < 4.6 \text{ TeV}$
 $-2.0 < y^* < 2.5, 1.3 < m_{jj} < 5 \text{ TeV}$
 $-2.5 < y^* < 3.0, 2 < m_{jj} < 5 \text{ TeV}$

Dijet $R=0.4, |y| < 3.0, y^* < 3.0$
 $-y^* < 0.5, 0.3 < m_{jj} < 4.3 \text{ TeV}$
 $-0.5 < y^* < 1.0, 0.3 < m_{jj} < 4.3 \text{ TeV}$
 $-1.0 < y^* < 1.5, 0.5 < m_{jj} < 4.6 \text{ TeV}$
 $-1.5 < y^* < 2.0, 0.8 < m_{jj} < 4.6 \text{ TeV}$
 $-2.0 < y^* < 2.5, 1.3 < m_{jj} < 5 \text{ TeV}$
 $-2.5 < y^* < 3.0, 2 < m_{jj} < 5 \text{ TeV}$



Inclusive jet production

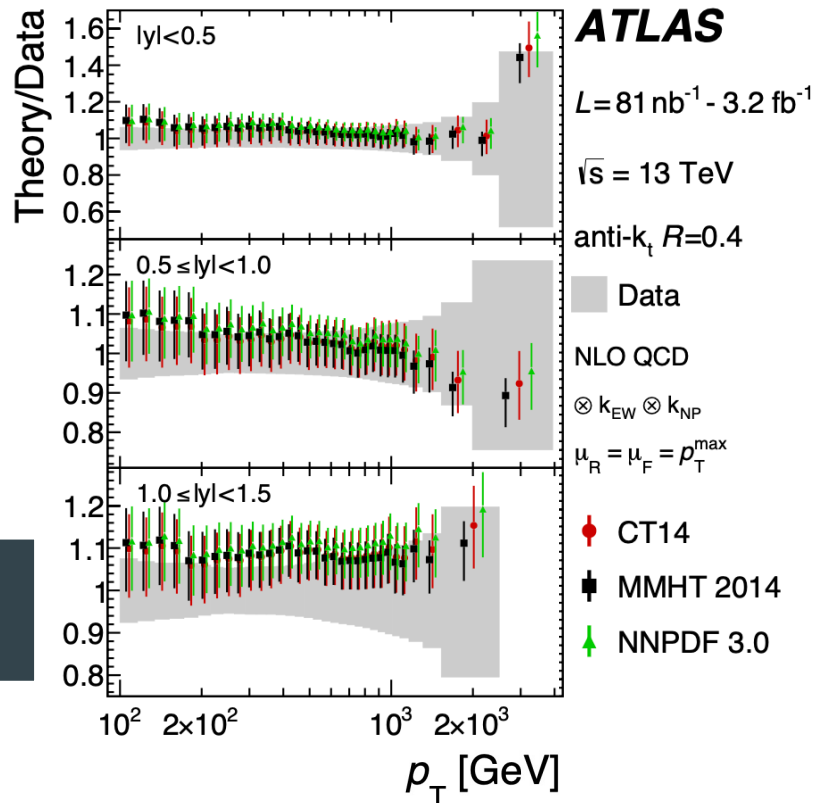
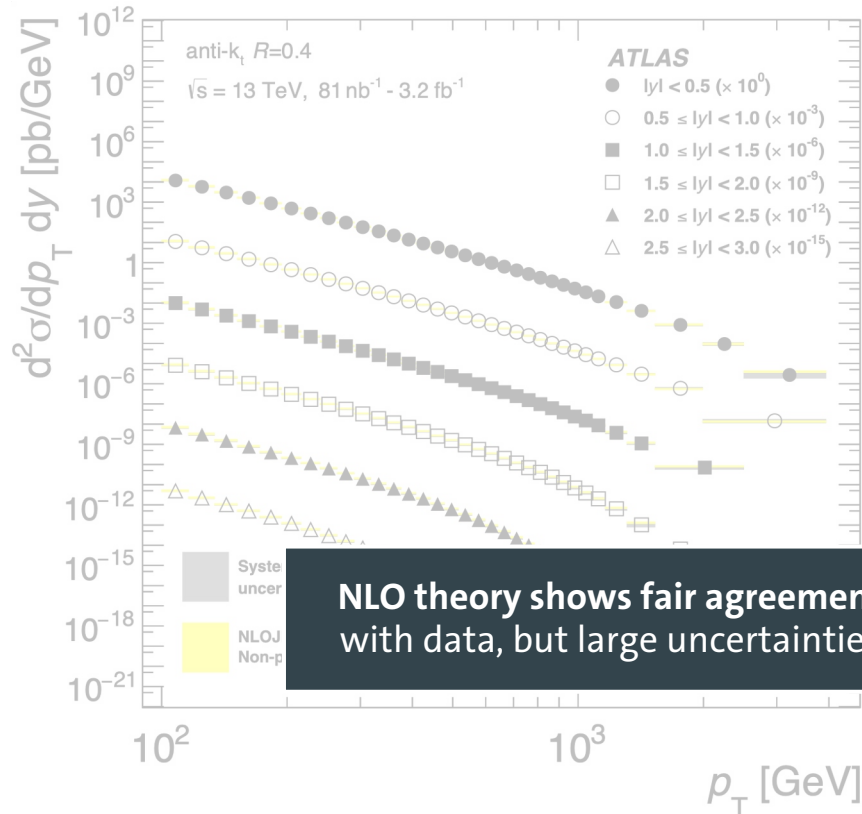
first results at 13 TeV



steeply falling spectrum
covering large p_T range

Inclusive jet production

first results at 13 TeV



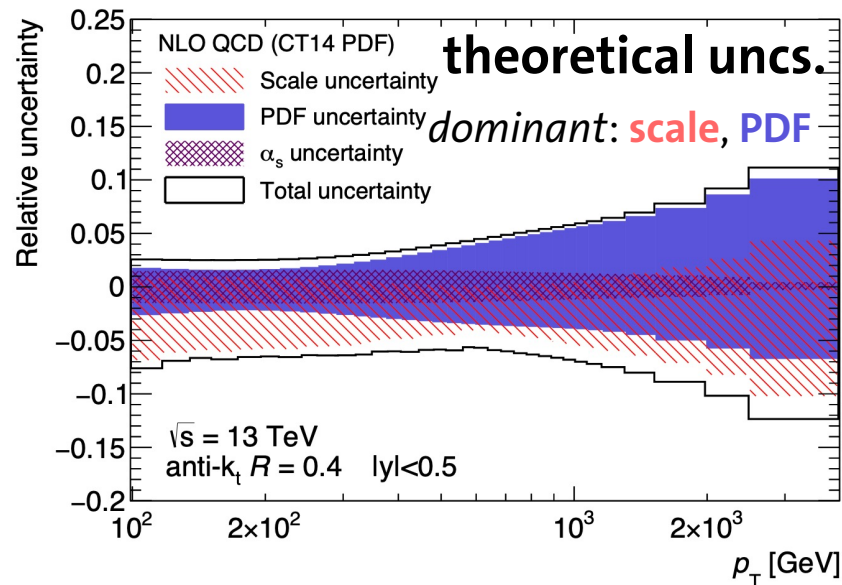
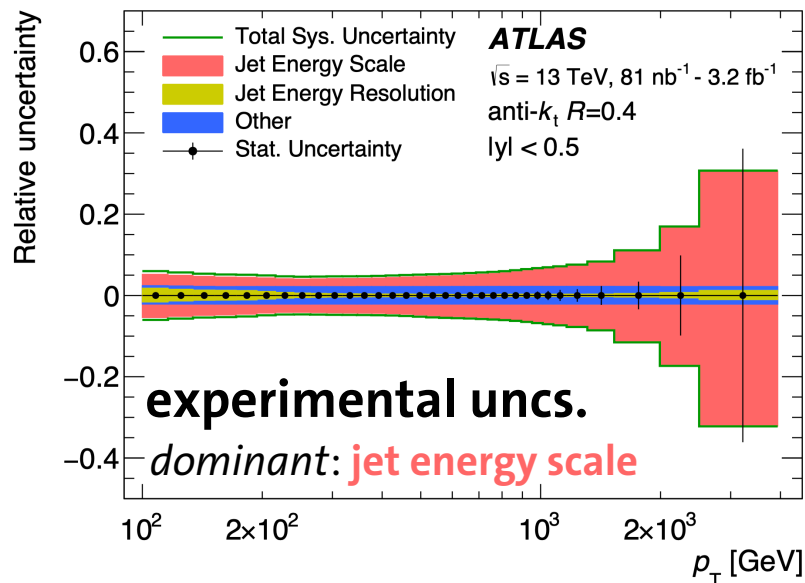
Inclusive jet production – uncertainties

first results at 13 TeV

[arXiv:1711.02692]
[JHEP 05 (2018) 195]



“scale” → missing higher orders in perturbation theory



improvement in experimental methods,
calibration to reduce uncertainties



increase in accuracy of theoretical
calculations + models

Inclusive jet production at $\sqrt{s} = 13$ TeV

[arXiv:2111.10431]

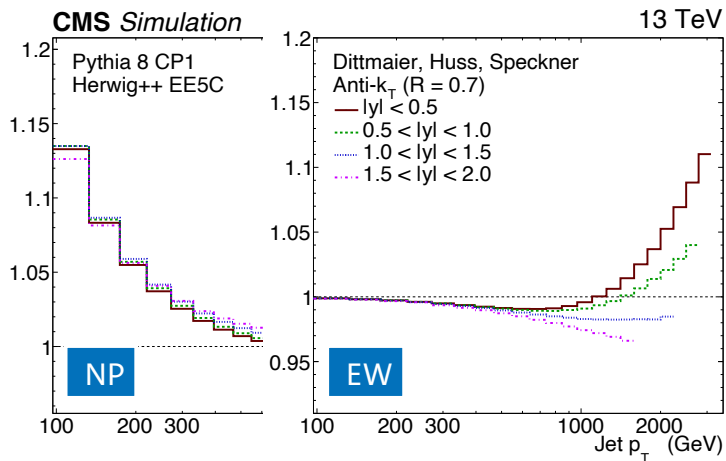
[JHEP 02 (2022) 142]

+ addendum [JHEP 12 (2022) 035]

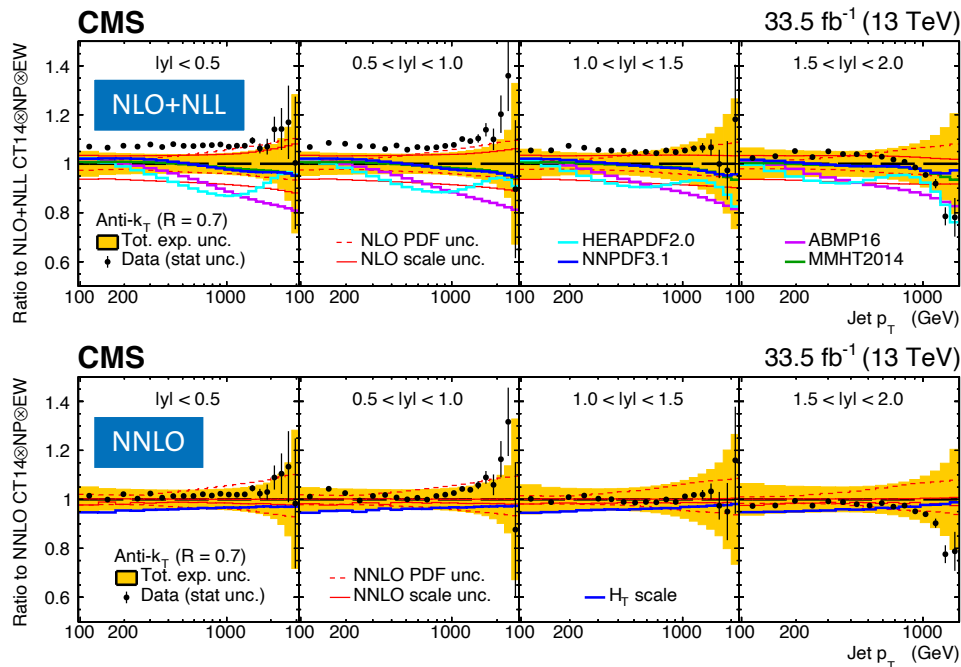


comparison to fixed-order pQCD theory at **NNLO** and **NLO+NLL**,
corrected for non-perturbative (**NP**)
and electroweak (**EW**) effects

improved agreement at NNLO



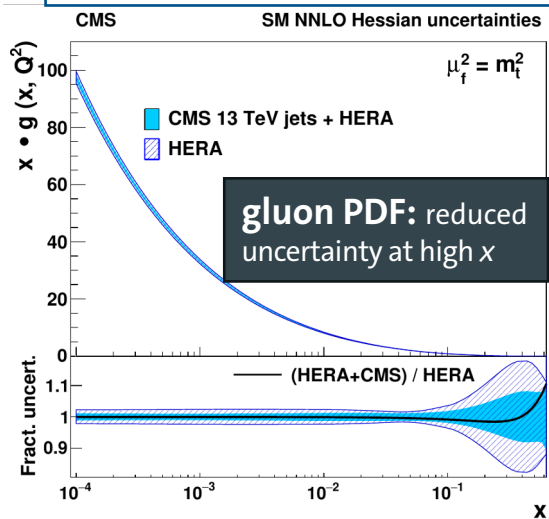
**theory corrections of >10%
in certain phase space regions**



Highlights

SM fits @ NNLO

PDFs + $\alpha_s(m_Z)$



$$\alpha_s(m_Z) = 0.1166 \pm 0.0014 \text{ (fit)}$$

$$\pm 0.0007 \text{ (model)}$$

$$\pm 0.0004 \text{ (scale)}$$

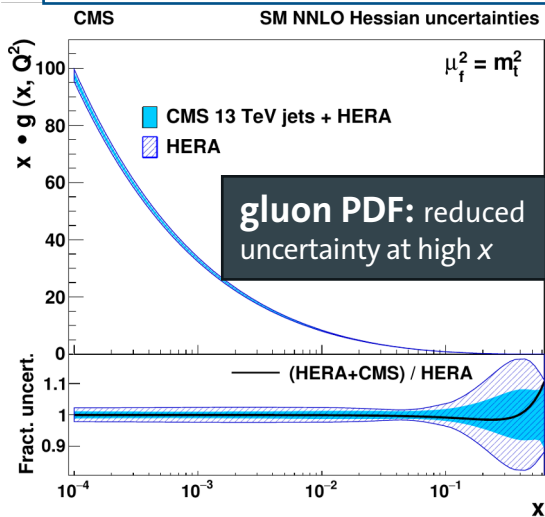
$$\pm 0.0001 \text{ (param.)}$$

**most precise NNLO result
from jet cross sections**

Highlights

SM fits @ NNLO

PDFs + $\alpha_s(m_Z)$



$\alpha_s(m_Z) = 0.1166 \pm 0.0014$ (fit)
 ± 0.0007 (model)
 ± 0.0004 (scale)
 ± 0.0001 (param.)

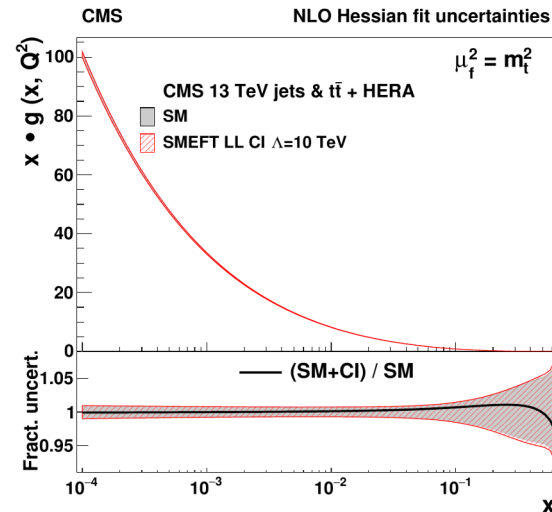
most precise NNLO result from jet cross sections

top quark mass in good agreement with previous CMS results using only $t\bar{t}$ data

$m_t^{(pole)}$ [GeV] = **170.4** ± 0.6 (fit)
 ± 0.1 (model)
 ± 0.1 (scale)
 ± 0.1 (param.)

combined fits
with other data sets

PDFs + $\alpha_s(m_Z)$ + $m_t^{(pole)}$



$\alpha_s(m_Z) = 0.1188 \pm 0.0017$ (fit)
 ± 0.0004 (model)
 ± 0.0025 (scale)
 ± 0.0001 (param.)

Highlights

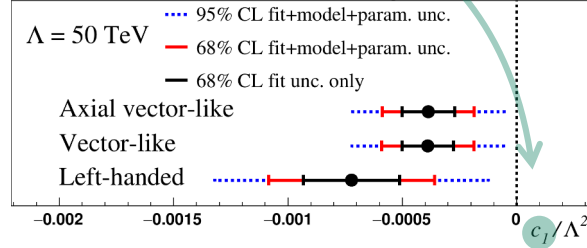


SMEFT constraints

constrain *Wilson coefficients* for SM extensions involving four-quark contact interactions

$$\mathcal{L}_{\text{SMEFT}} = \mathcal{L}_{\text{SM}} + \frac{2\pi}{\Lambda^2} \sum_{n \in \{1,3,5\}} c_n O_n$$

CMS SMEFT NLO 13 TeV jets & $t\bar{t}$ + HERA

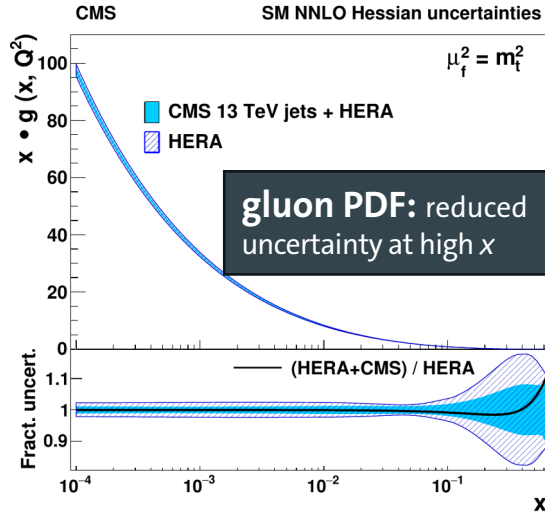


top quark mass in good agreement with previous CMS results using only $t\bar{t}$ data

$$m_t^{(\text{pole})} [\text{GeV}] = 170.4 \pm 0.6 \text{ (fit)} \\ \pm 0.1 \text{ (model)} \\ \pm 0.1 \text{ (scale)} \\ \pm 0.1 \text{ (param.)}$$

SM fits @ NNLO

PDFs + $\alpha_s(m_Z)$

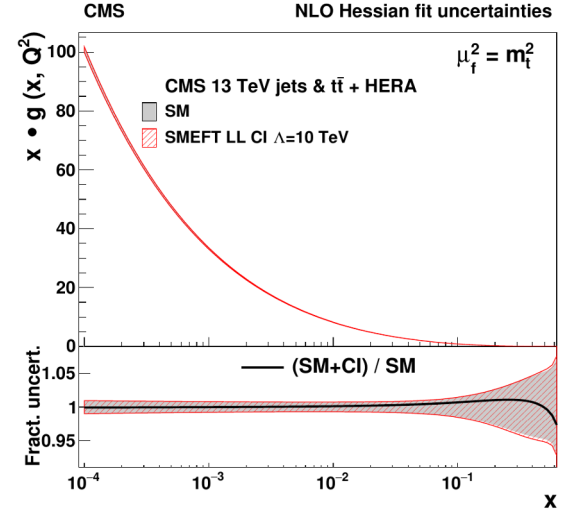


$$\alpha_s(m_Z) = 0.1166 \pm 0.0014 \text{ (fit)} \\ \pm 0.0007 \text{ (model)} \\ \pm 0.0004 \text{ (scale)} \\ \pm 0.0001 \text{ (param.)}$$

most precise NNLO result
from jet cross sections

combined fits
with other data sets

PDFs + $\alpha_s(m_Z)$ + $m_t^{(\text{pole})}$

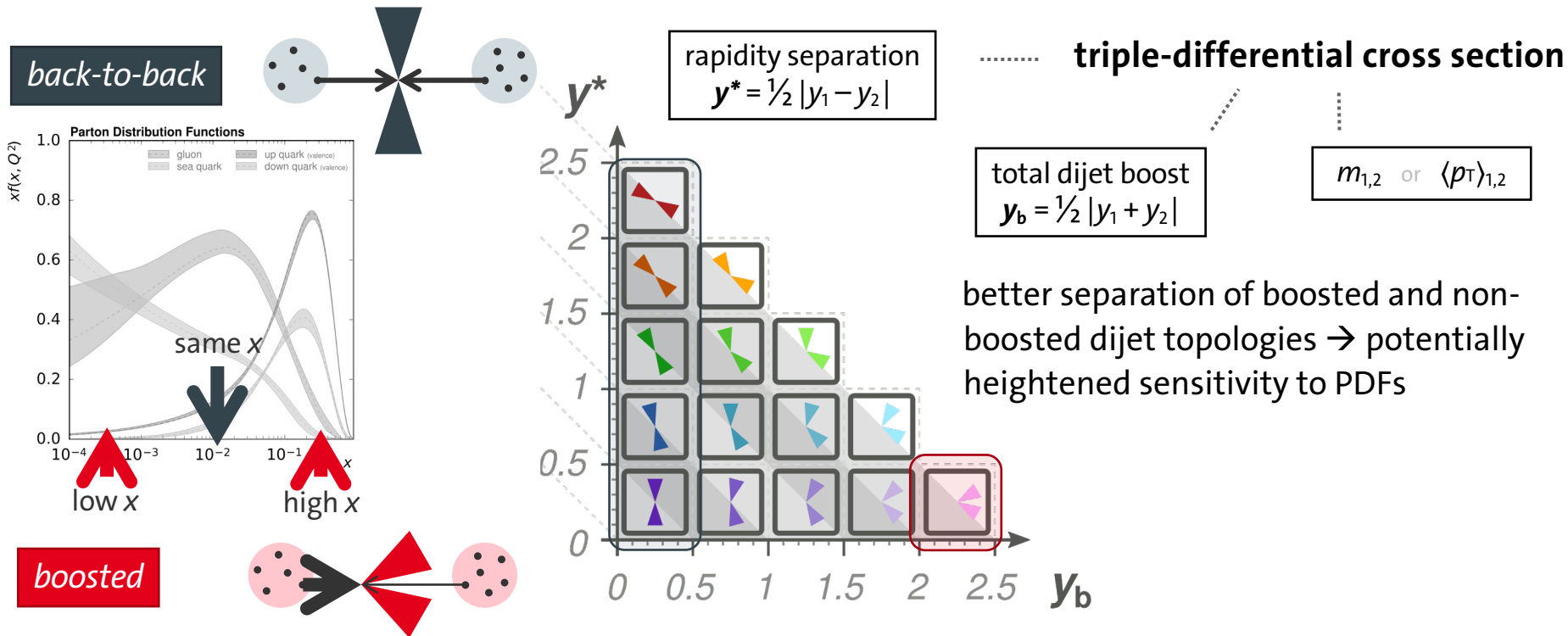


jet data “pins down” PDFs + $\alpha_s(m_Z)$
increased sensitivity to other parameters

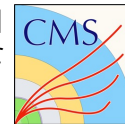
$$\alpha_s(m_Z) = 0.1188 \pm 0.0017 \text{ (fit)} \\ \pm 0.0004 \text{ (model)} \\ \pm 0.0025 \text{ (scale)} \\ \pm 0.0001 \text{ (param.)}$$

Dijet production

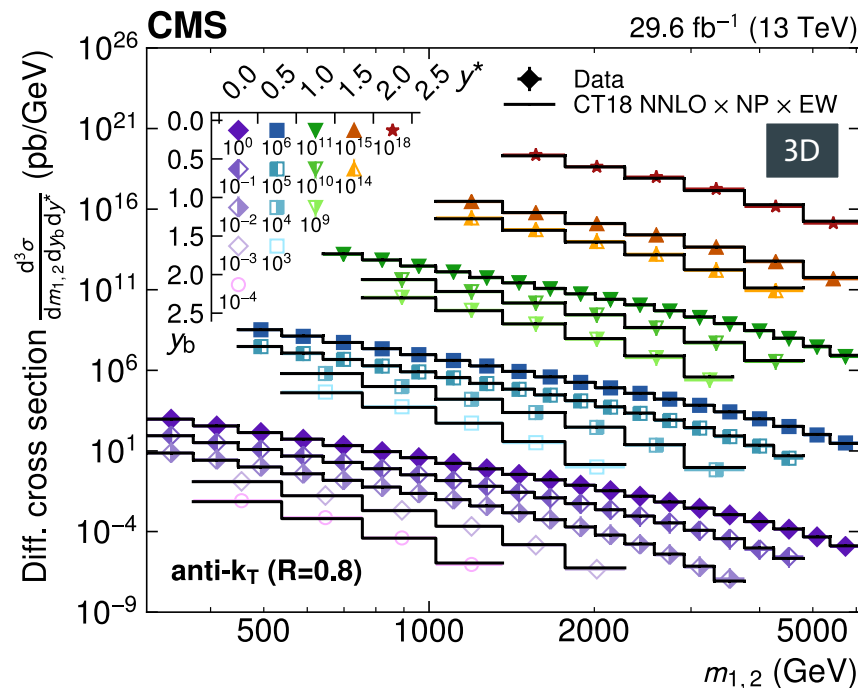
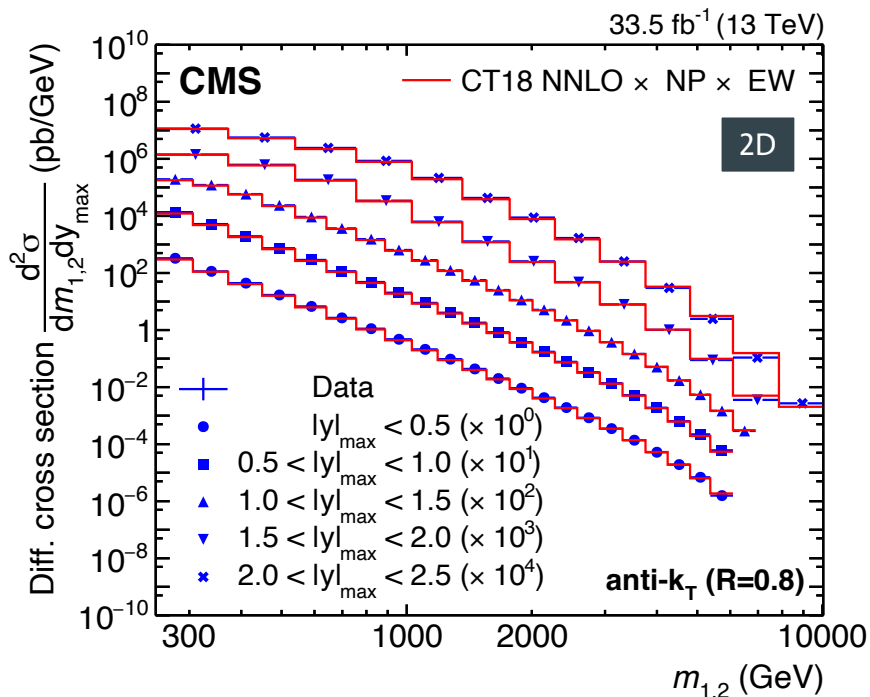
exploit topology of two hardest jets to enhance sensitivity to PDFs



Dijet cross sections at 13 TeV



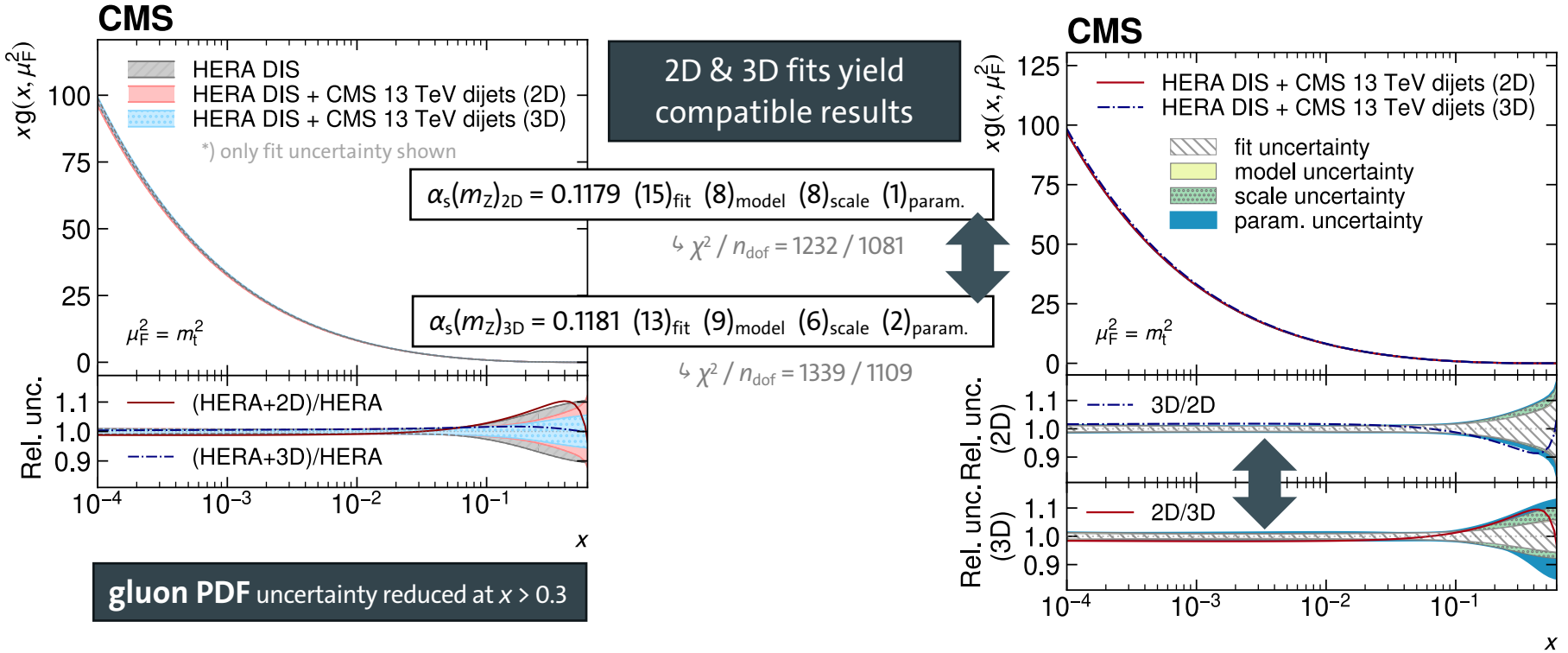
- **double- (2D) & triple-differential (3D) cross section vs. dijet invariant mass $m_{1,2}$**
- comparison to fixed-order theory at **NNLO** pQCD from **NNLOJET + fastNLO**



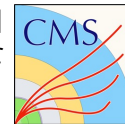
Dijet cross sections at 13 TeV



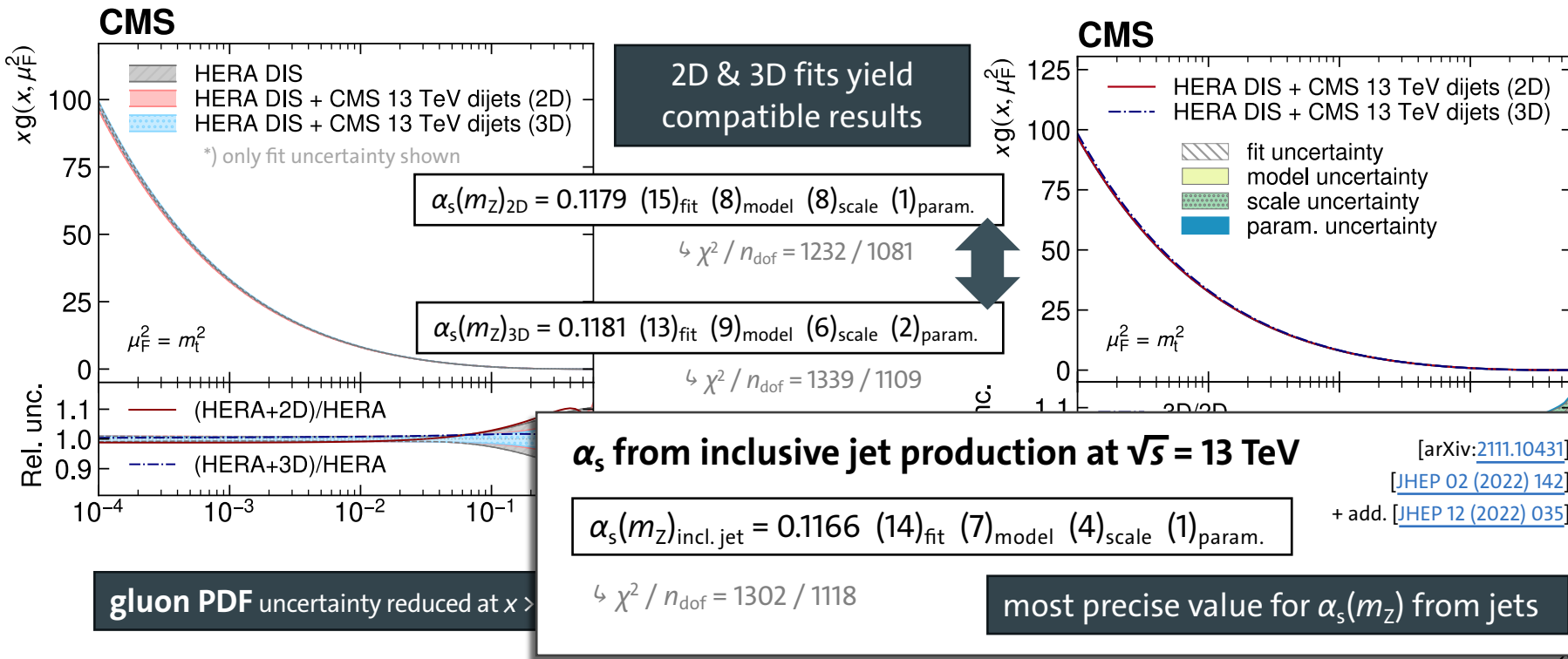
PDFs and $\alpha_s(m_Z)$ determined simultaneously in fits to CMS dijet & HERA DIS data



Dijet cross sections at 13 TeV



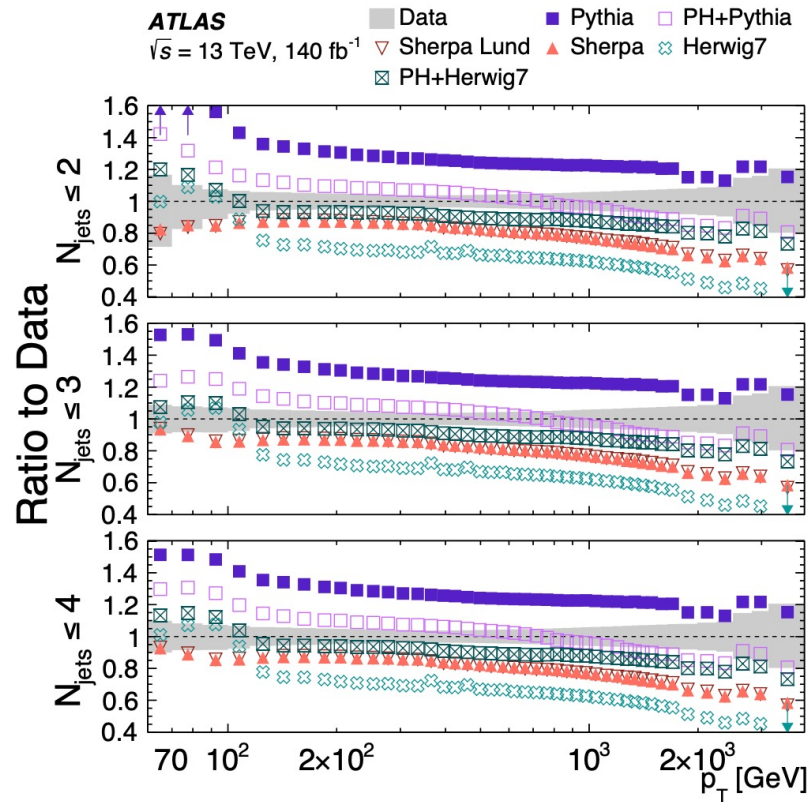
PDFs and $\alpha_s(m_Z)$ determined simultaneously in fits to CMS dijet & HERA DIS data



Jet cross sections vs. multiplicity

- differential cross section measured in bins of **jet multiplicity** N_{jets} from 140 fb^{-1} of data
- inclusive jet and dijet cross sections as a function of p_T and $H_{T2} = p_{T,1} + p_{T,2}$
- comparison to MC generators & fixed-order theory at NLO pQCD

no MC describes data in entire phase space,
best overall agreement from *Sherpa*

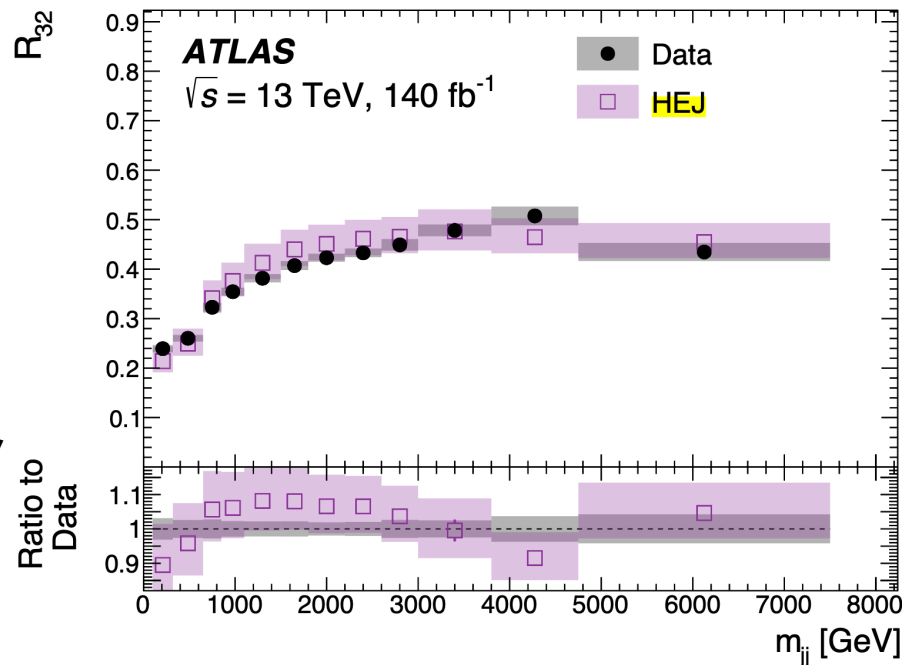


Jet cross section ratios

- **ratios** measured between multiplicity bins, benefit from cancellation of systematic uncertainties, e.g.

$$R_{32} = \frac{\sigma(N_{\text{jets}} \leq 3)}{\sigma(N_{\text{jets}} \leq 2)}$$

- comparison to NNLO theory using **High Energy Jets** theoretical framework for calculating logarithmic corrections to all orders in α_s

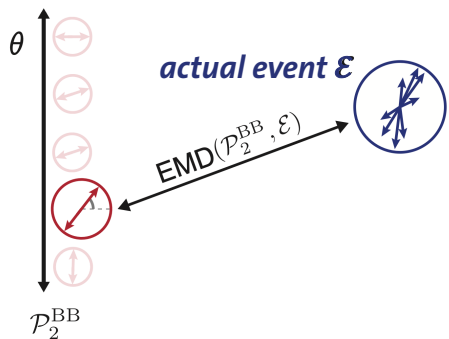


Multijet event isotropies



- **isotropies** = event shape variables that quantify the distance from a “symmetric radiation pattern”
- minimization of *distance metric* to **reference geometries** (dipole, cylinder, ring, etc.)

example:
dipole



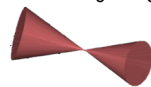
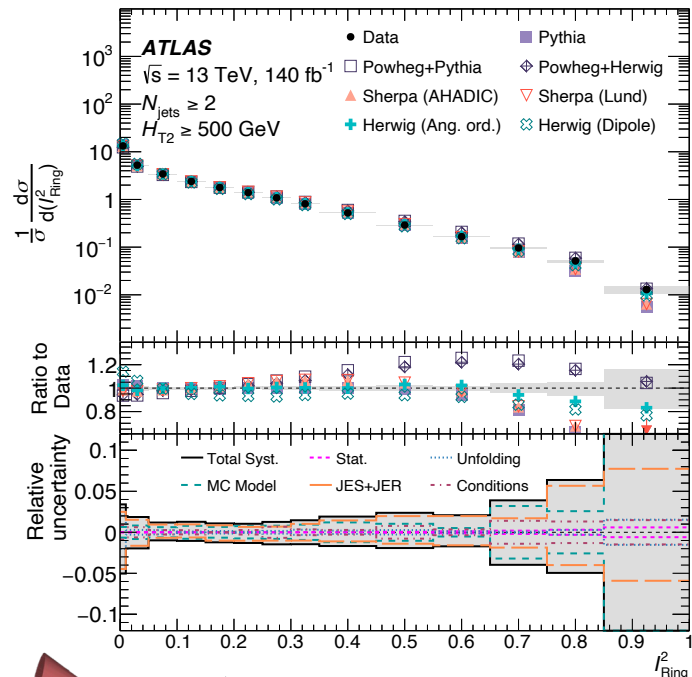
Energy-Mover's Distance

$$\text{EMD}_\beta(\mathcal{E}, \mathcal{E}') = \min_{\{f_{ij} \geq 0\}} \sum_{i=1}^M \sum_{j=1}^{M'} f_{ij} \theta_{ij}^\beta,$$

- data/theory best for balanced **dijet**-like configuration, **deteriorates** at high isotropy
- explore remote areas of QCD phase space, useful as input to **MC tuning**

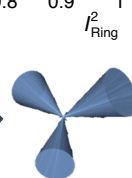
example: I_{Ring}^2

[arXiv:2305.16930]
[JHEP 10 (2023) 060]



← more **dijet**-like

more **symm. trijet**-like →



Jet azimuthal correlations

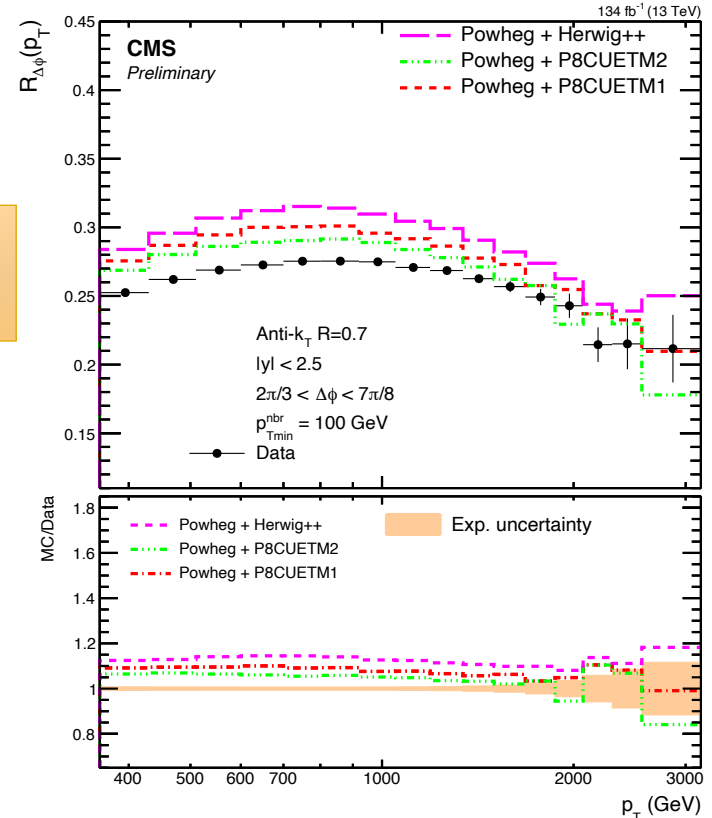


- observable $R_{\Delta\phi}$ defined via the **number of neighboring jets** within a specified interval of **angular distance $\Delta\phi$**

$$R_{\Delta\phi}(p_T) = \frac{\sum_{i=1}^{N_{\text{jet}}(p_T)} N_{\text{nbr}}^{(i)}(\Delta\phi, p_{T\text{min}}^{\text{nbr}})}{N_{\text{jet}}(p_T)}$$

ratio observable
→ many systematic uncertainties cancel

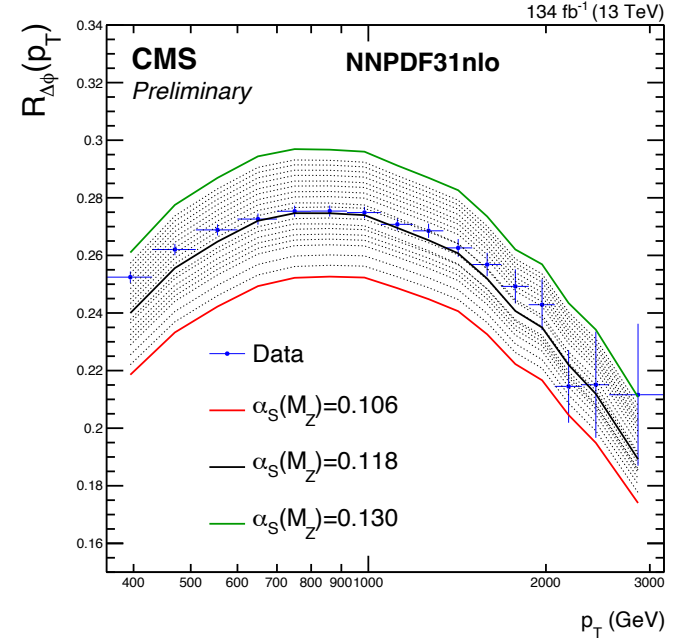
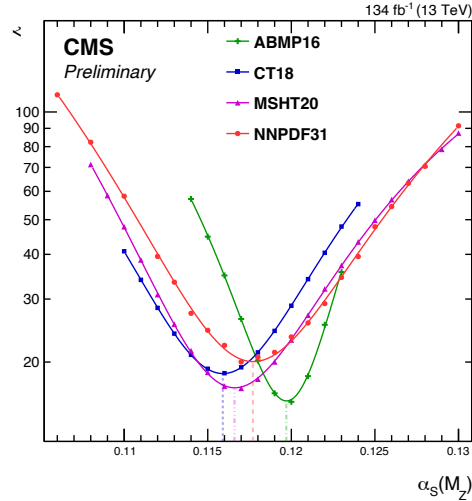
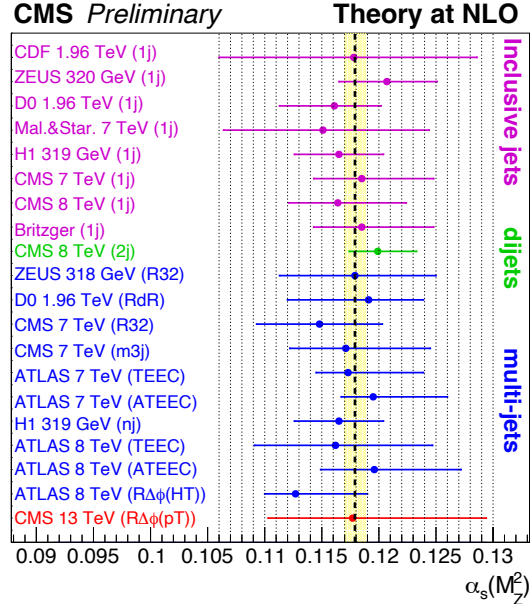
- interval $\left(\frac{2\pi}{3} < \Delta\phi < \frac{7\pi}{8}\right)$ separates dijet topologies from 3+ jets → **sensitivity to $\alpha_s(m_Z)$**



Jet azimuthal correlations



- extraction of $\alpha_s(m_Z)$ from comparison to fixed-order pQCD predictions at **NLO** using several global PDF sets + nonperturbative & electroweak corrections

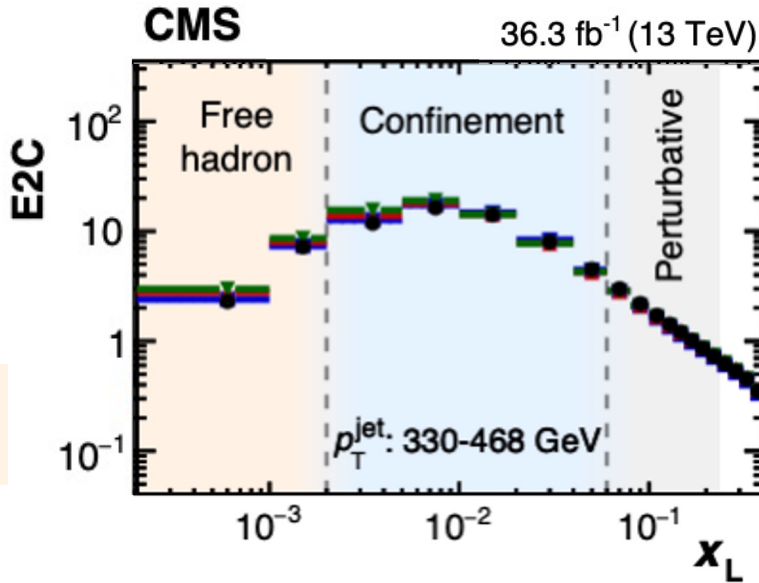


$$\alpha_s(m_Z)_{\text{NLO}} = 0.1177 (13)_{\text{exp}} \left(\begin{matrix} +116 \\ -73 \end{matrix} \right)_{\text{theo.}}$$

Energy correlators (EECs)



- **substructure observables** that describe the correlations of kinematic properties of particles inside jets, weighted by energy $\rightarrow E_i E_j / E^2$ or $E_i E_j E_k / E^3$
- calculated based on **pairs** (E2C) or **triplets** (E3C) of constituent particles
- ordered by **angular separation** $x_L \rightarrow$ probe timescale of hadron formation



wide angle splittings,
perturbation theory

small angle splittings,
non-interacting hadrons

Energy correlators (EECs)

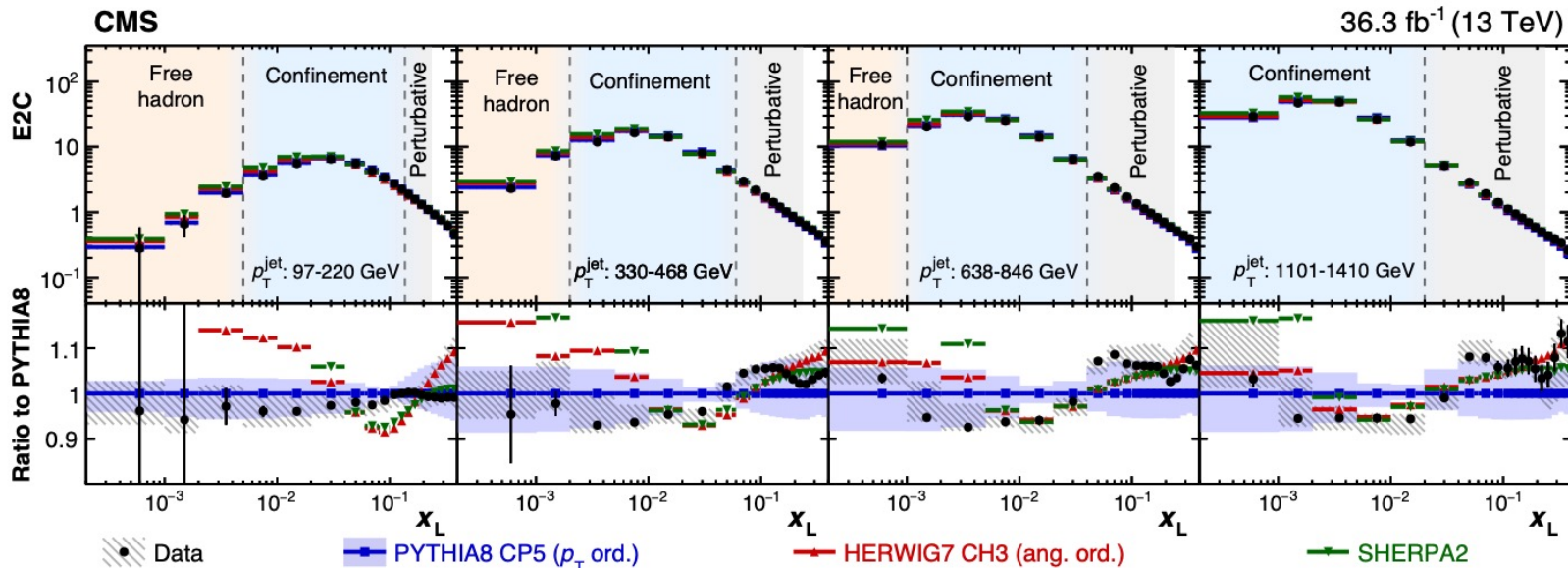


- EECs measured in bins of jet p_T and compared to predictions from MC generators

PYTHIA 8, **Herwig 7** and **SHERPA 2**

best overall description

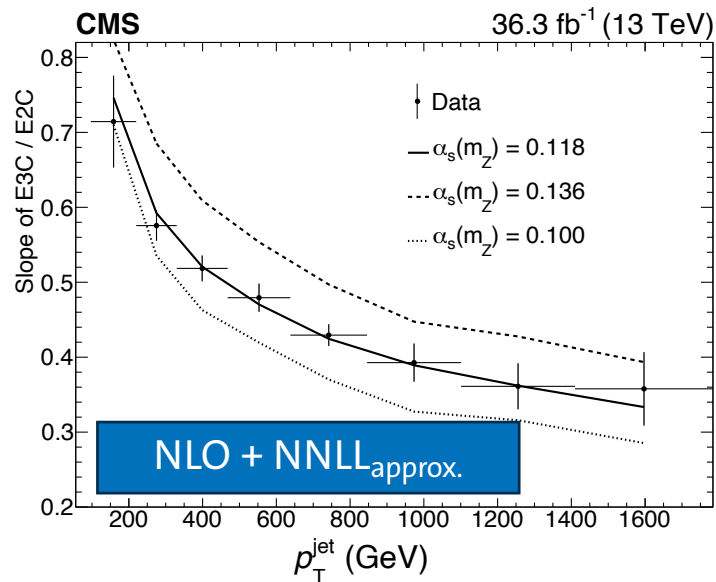
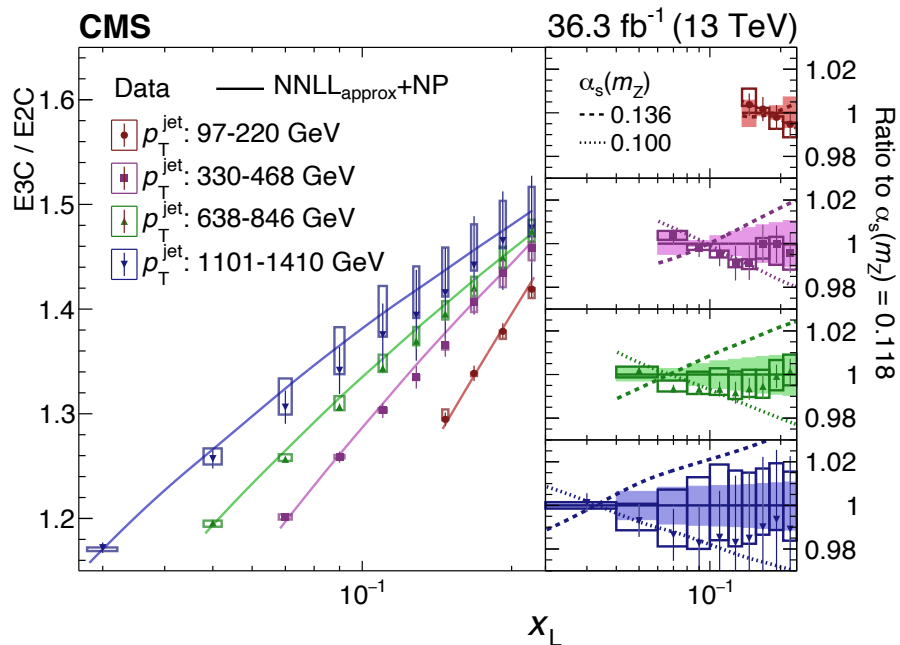
perform better in some regions



Strong coupling from EECs

ratio of E3C and E2C sensitive to $\alpha_s(m_Z)$:

- approx. linear in $\alpha_s \ln x_L$
- PDF dependence largely suppressed



$$\alpha_s(m_Z)_{\text{EEC}} = 0.1229 \left(\begin{array}{c} +14 \\ -12 \end{array} \right)_{\text{stat.}} \left(\begin{array}{c} +23 \\ -36 \end{array} \right)_{\text{exp.}} \left(\begin{array}{c} +30 \\ -33 \end{array} \right)_{\text{theo.}}$$

most precise $\alpha_s(m_Z)$ from substructure

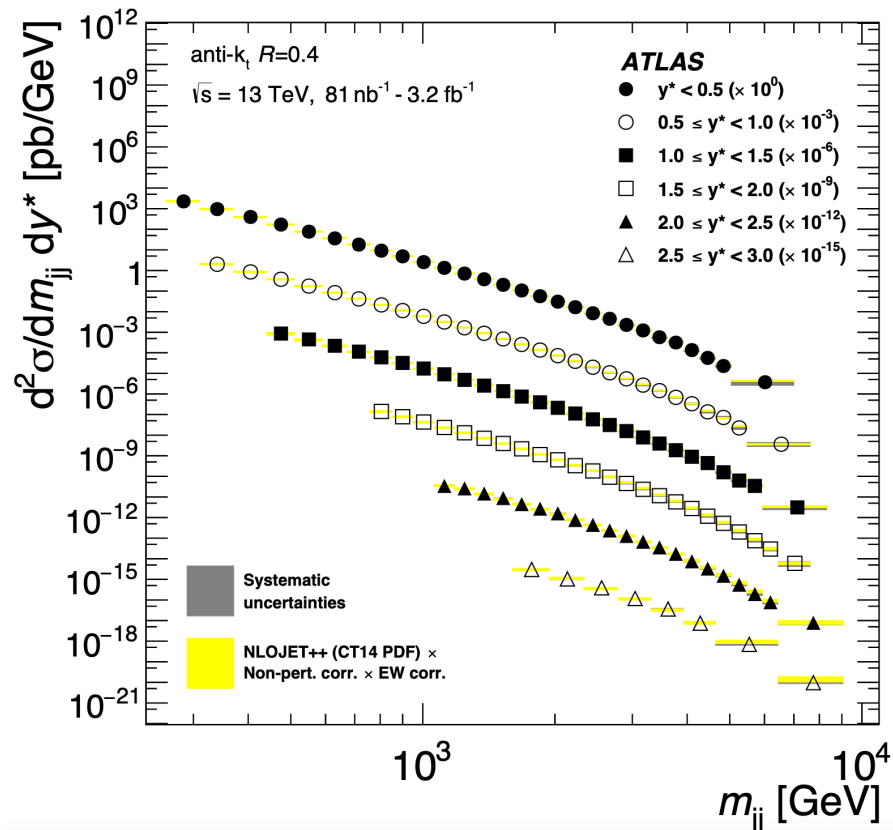
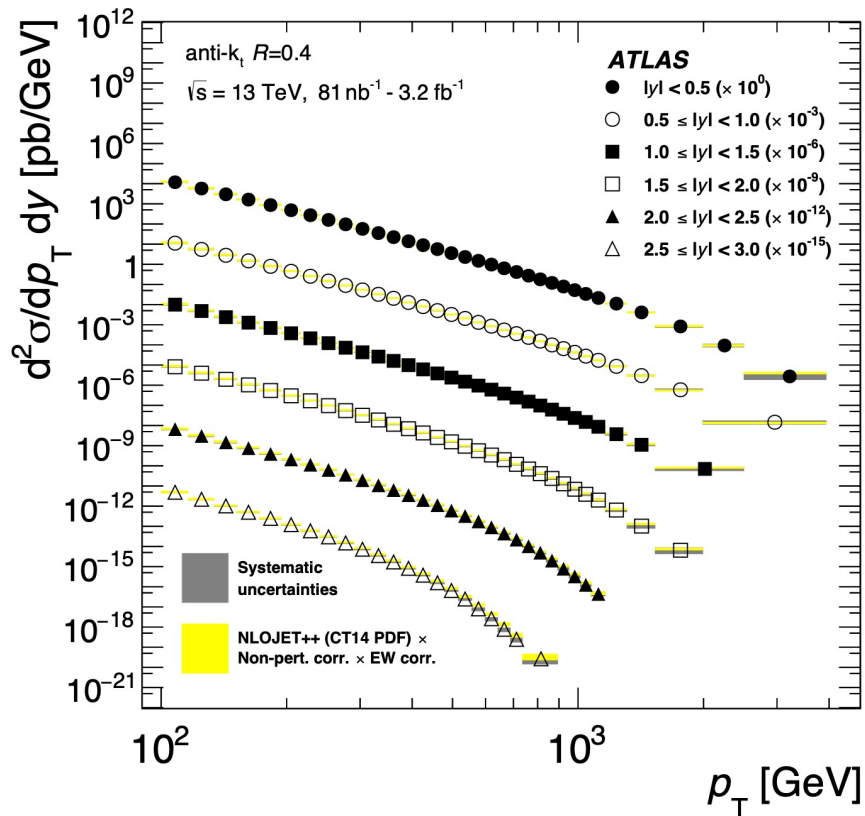
Summary

- presented recent results on **jet measurements** from the **ATLAS & CMS** collaborations
- diverse measurement programs, targeting various observables, e.g. **jet cross sections, event shapes, jet substructure**
- precision measurements provide essential input for improving our knowledge of the Standard Model, esp. for determinations of **strong coupling $\alpha_s(m_Z)$ and parton distributions**
- large accessible phase space, useful for improvement and tuning of **MC models**
- improved experimental techniques + fixed-order predictions up to and beyond **NNLO** accuracy in pQCD are instrumental for improving precision and reducing systematic uncertainties

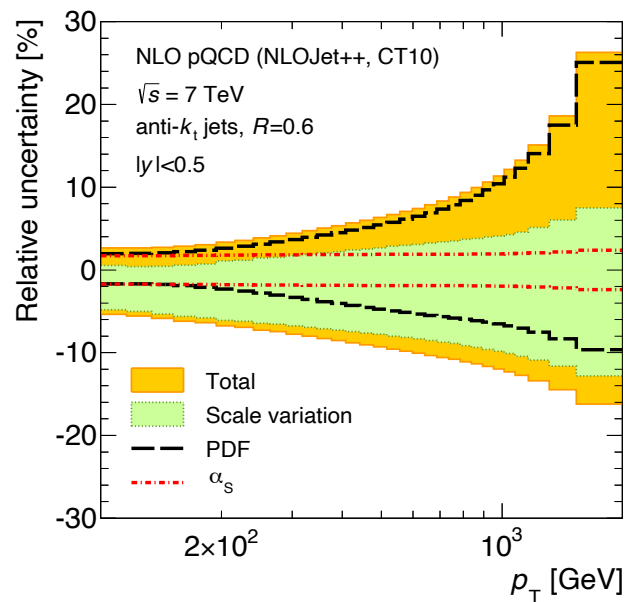
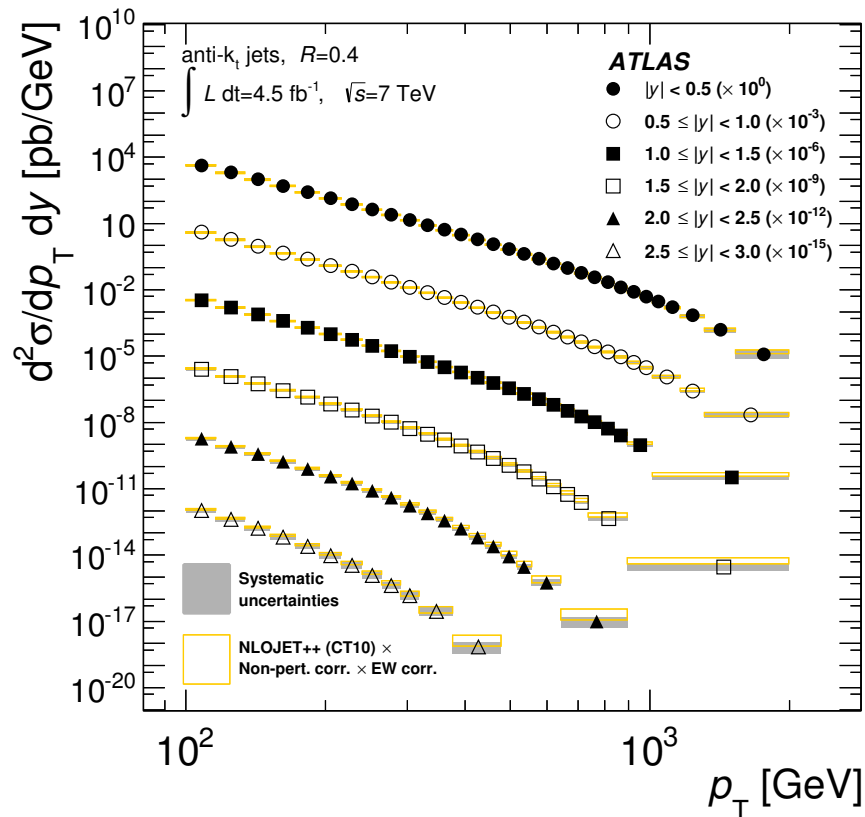
Thank you for your attention!

Backup

ATLAS inclusive jets 13 TeV



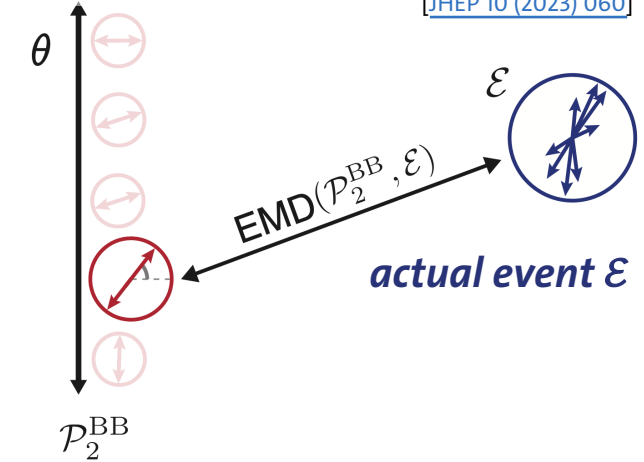
ATLAS inclusive jets 7 TeV



Multijet event isotropies

- **isotropies** = event shape variables that quantify the distance from a “symmetric radiation pattern”
- infrared- and collinear-safe + complementary to traditional variables like **thrust**, **sphericity**, **spherocity**
- obtained by minimization of **distance metric** to isotropic reference geometries (cylindrical, spherical)

example reference geometry: **dipole**



Energy-Mover's Distance

$$\text{EMD}_\beta(\mathcal{E}, \mathcal{E}') = \min_{\{f_{ij} \geq 0\}} \sum_{i=1}^M \sum_{j=1}^{M'} f_{ij} \theta_{ij}^\beta,$$

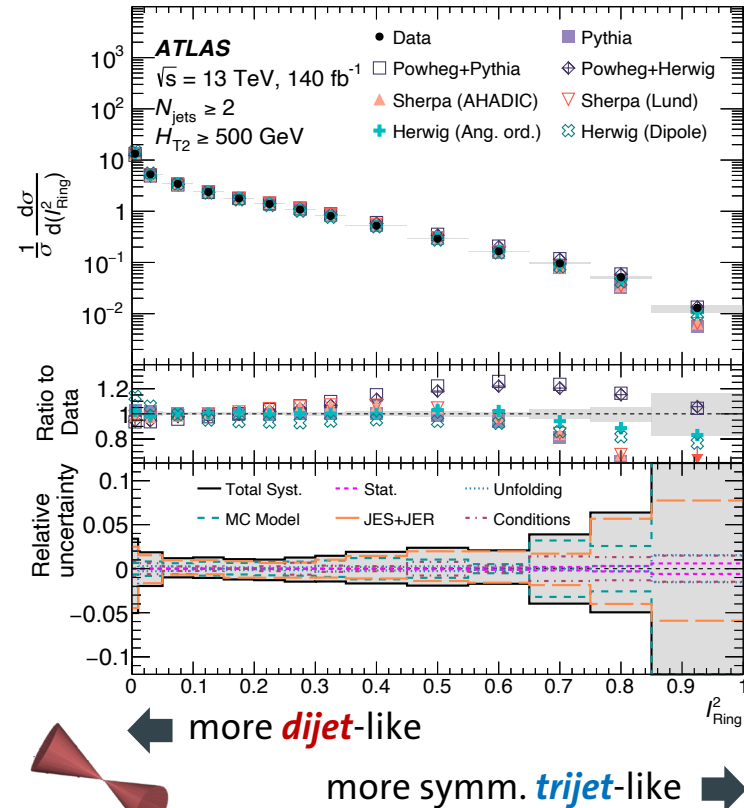
sum over object pairs \nearrow f_{ij} (energy transfer) \uparrow θ_{ij} (ground measure (e.g. angle)) \downarrow β (angular weighting exponent)

Multijet event isotropies

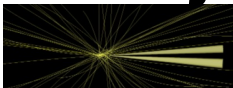
- measured in bins of **jet multiplicity** (N_{jet}) and **scalar sum of two leading jets' transverse momenta** (H_{T2})
- data best described by simulation in balanced, ***dijet***-like configuration (low isotropy), ***deterioration*** at high isotropy
- explore remote areas of QCD phase space, useful as inputs to ***MC tuning***

example: I_{Ring}^2

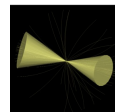
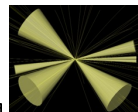
[arXiv:2305.16930]
[JHEP 10 (2023) 060]



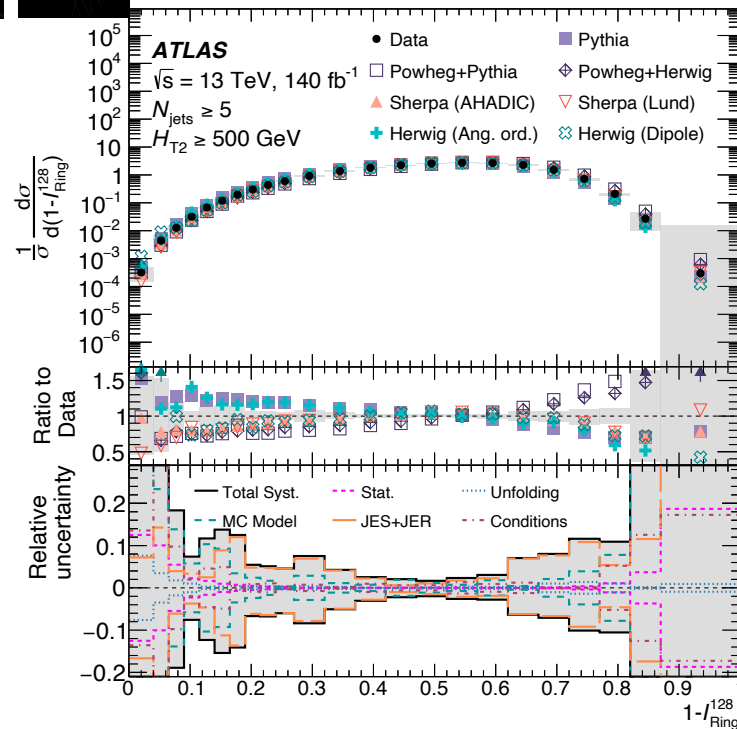
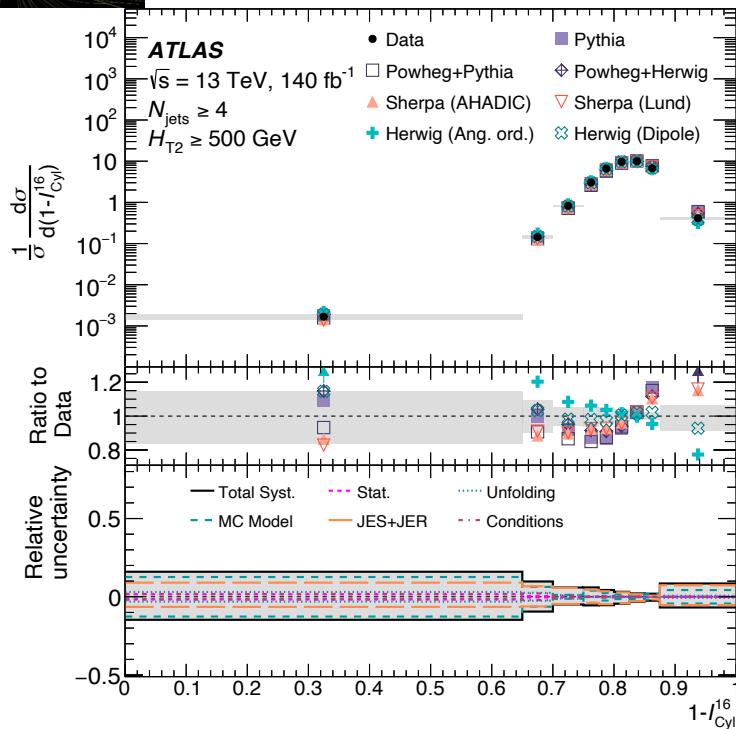
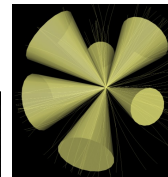
Multijet event isotropies



forward dijet \leftrightarrow isotropic multijet



balanced dijet \leftrightarrow isotropic multijet



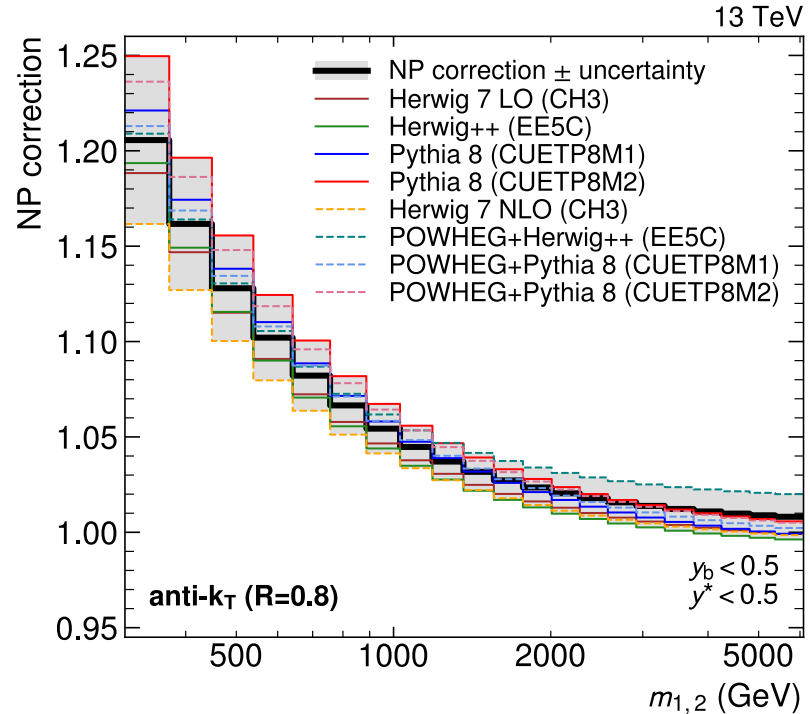
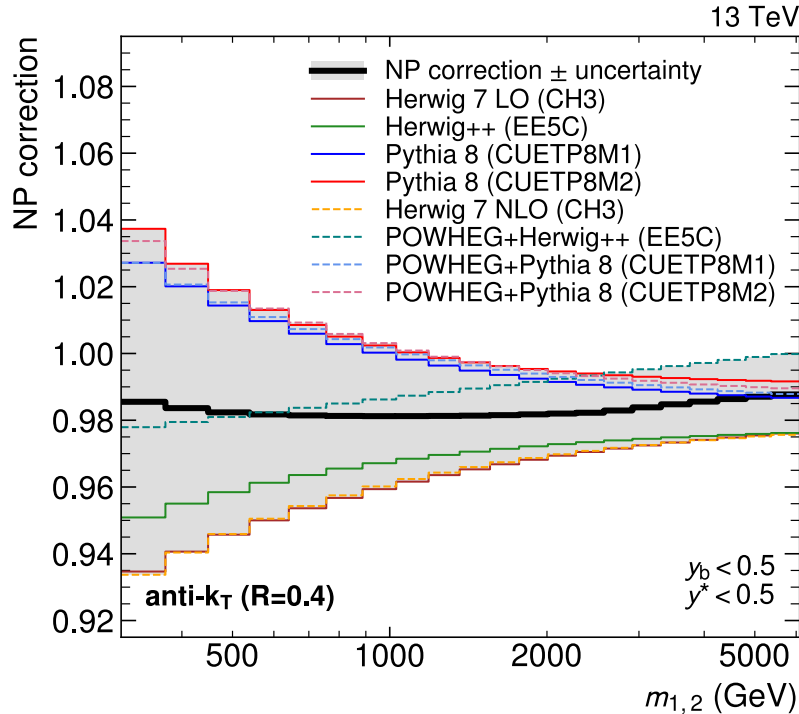
some isotropy shapes not described by any MC generator

Multidifferential dijet cross sections

[arXiv:[2312.16669](https://arxiv.org/abs/2312.16669)]
Submitted to EPJC



nonperturbative (NP) corrections

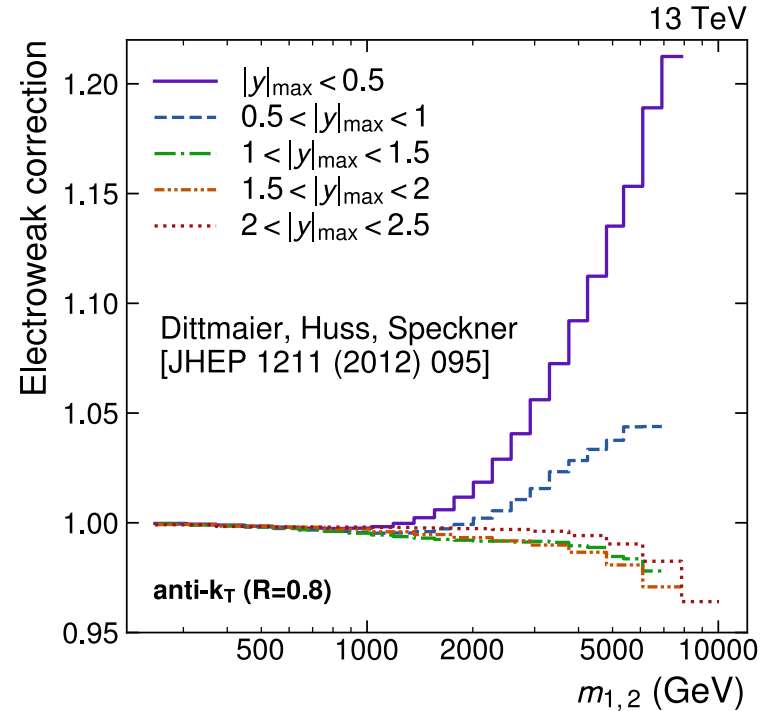
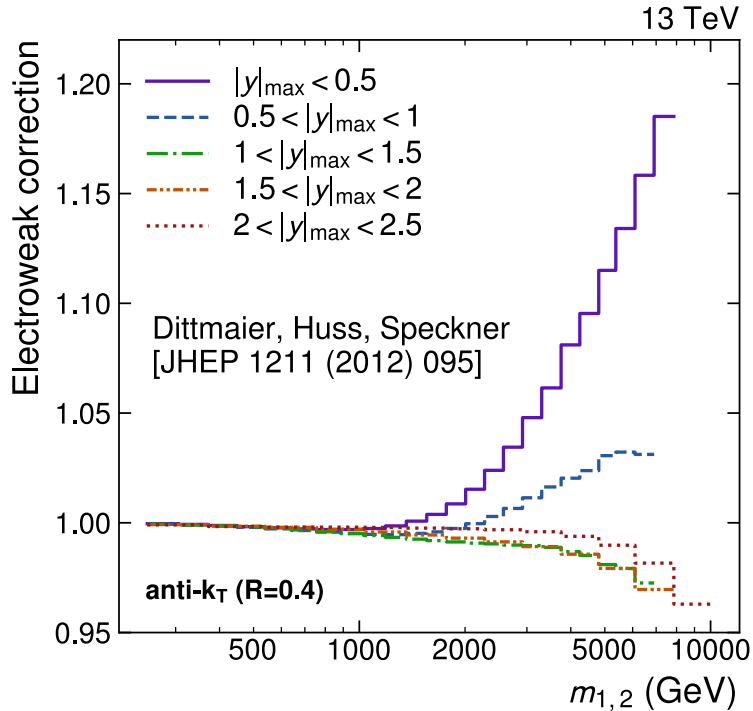


Multidifferential dijet cross sections

[arXiv:2312.16669]
Submitted to EPJC

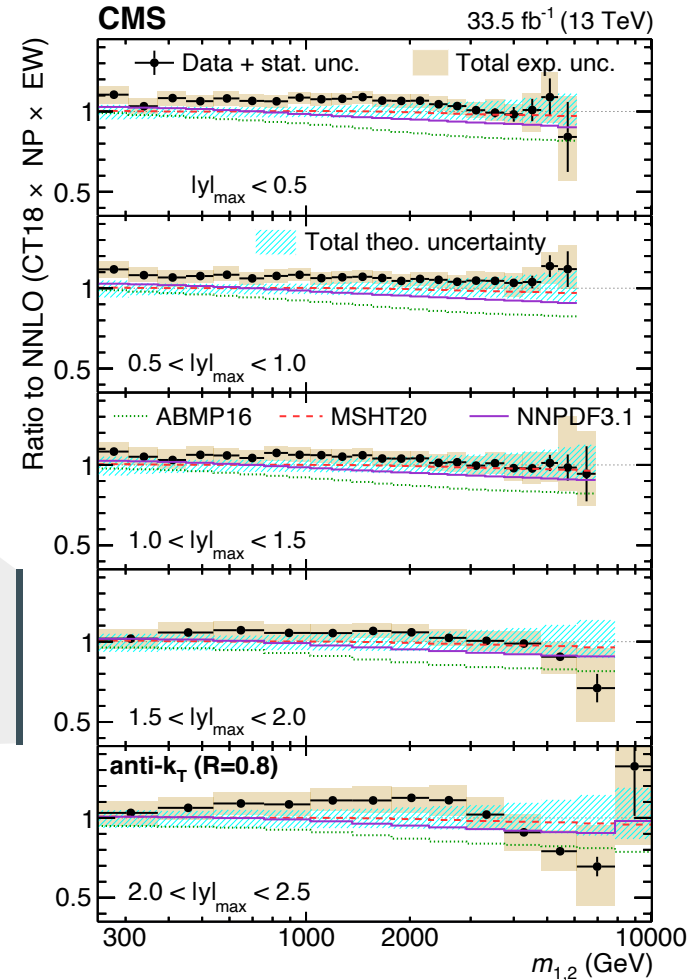
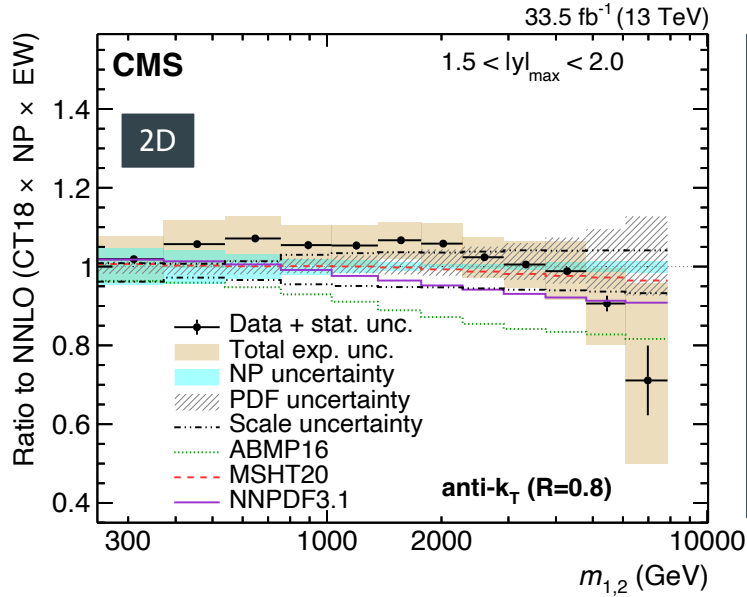


electroweak corrections



Multidifferential dijet cross sections

comparison to fixed-order theory predictions @ NNLO \times nonperturbative, electroweak corrections



Multidifferential dijet cross sections

comparison to fixed-order theory predictions @ NNLO ×
nonperturbative, electroweak corrections

